J. Membrane Biol. 152, 223–233 (1996)

The Journal of
Membrane
Biology

Ion Channel Permeable for Divalent and Monovalent Cations in Native Spinach Thylakoid Membranes

I.I. Pottosin*, G. Schönknecht
Julius-von-Sachs Institut für Biowissenschaften der Universität Würzburg, Mittlerer Dallenbergweg 64, D-97082 Würzburg, Germany

Received: 26 December 1995/Revised: 17 April 1996

Abstract. A cation-selective channel was characterized in isolated patches from osmotically swollen thylakoids of spinach (*Spinacea oleracea*). This channel was permeable for K^+ as well as for Mg^{2+} and Ca^{2+} but not for Cl^-. When K^+ was the main permeant ion (symmetrical 105 mM KCl) the conductance of the channel was about 60 pS. The single channel conductance for different cations followed a sequence $K^+ > Mg^{2+} \geqslant Ca^{2+}$. The permeabilities determined by reversal potential measurements were comparable for K^+, Ca^{2+}, and Mg^{2+}. The cation channel displayed bursting behavior. The total open probability of the channel increased at more positive membrane potentials. Kinetic analysis demonstrated that voltage dependence of the total open probability was determined by the probability of bursts formation while the probability to find the channel in open state within a burst of activity was hardly voltage-dependent. The cation permeability of intact spinach thylakoids can be explained on the single channel level by the data presented here.

Key words: Cation channel — K^+, Ca^{2+} and Mg^{2+} permeability — Voltage gating — Patch-clamp — Thylakoid membrane — Spinach

Introduction

Light-driven uptake of H^+ into thylakoids occurs in parallel with passive efflux of cations and influx of anions. As a result, the steady-state electrical potential difference across the thylakoid membrane is only about −10 mV, whereas large acidification of the thylakoid lumen by 2–3 pH units is observed (Bulychev et al., 1972; Junge & Jackson, 1982; Remiš, Bulychev & Kurella, 1986). Anions (Cl^- and NO_3^-) are likely to be transported through the thylakoid membrane via the voltage-dependent anion channel (Schönknecht et al., 1988). Recent patch-clamp studies have shown that this channel is a highly conserved component of the thylakoid membrane in both higher plants and green algae (Pottosin & Schönknecht, 1995*a*,*b*). Because of its high anion over cation selectivity a significant transport of cations through the thylakoid anion channel can be excluded. There is, nevertheless, a large body of evidence obtained especially on spinach, the most popular object of photosynthesis studies for a significant contribution of Mg^{2+} and/or K^+ to the light-induced ion fluxes across the thylakoid membrane (e.g., Dilley & Vernon, 1965; Hind, Nakatani & Izawa, 1974). Our recent patch-clamp measurements with spinach thylakoids revealed in addition to the anion channel, also observed in other plant species, a cation-selective channel (Pottosin & Schönknecht, 1995*b*).

In this study we attempted to answer the question, which among the physiologically significant ions as K^+, Cl^-, Mg^{2+} and Ca^{2+} are transported through the cation channel. We explored also the dependence of single channel kinetics on the membrane voltage.

Materials and Methods

Preparation

Spinach (*Spinacea oleracea*) sort Matador was grown in a greenhouse at 20–24°C under 10/14 hr day/night cycle. Leaves of 7–9-week-old plants were used for experiments. Spinach chloroplasts were isolated mechanically and thylakoid membranes were swollen in hypotonic solution as described previously (Pottosin & Schönknecht, 1995*a*). This procedure resulted in formation of large (10–15 μm) spherical blebs

* *On leave from:* The Institute for Cell Biophysics, Russian Academy of Sciences, 142292 Puschino, Moscow region, Russia

Correspondence to: G. Schönknecht

(swollen thylakoids) which were used for further patch-clamp recordings.

Patch-clamp Measurements

Micropipettes were prepared as described previously (Pottosin & Schönknecht, 1995*a*). After fire polishing, the resistance of patch pipettes filled with ''100 KCl'' solution (*see* Table) was 10–15 MΩ. The reference AgCl electrode was connected to the batch via an agar bridge filled with 100 mM KCl. Electrical measurements were performed using an Axopatch 200A Integrating Patch-Clamp amplifier (Axon Instruments, Foster City, CA). Tight seals (5–20 GΩ) between glass microelectrode and thylakoid membrane were achieved by applying a light suction pulse. All experiments were performed in the inside-out patch configuration (Hamill et al., 1981) which means the lumenal side of the thylakoid membrane was exposed to the bath. The convention of current and voltage was according to Azzone et al. (1993), i.e., the sign of voltage refers to the stromal side (pipette voltage for inside-out patches). Positive currents represent an efflux of cations from the pipette to the intrathylakoid side.

Liquid Junction Potential Correction

Whenever solutions with two different ion compositions are in contact, a liquid junction potential (V_{LJ}) is developed between them. A proper correction of V_{LJ} is necessary for the determination of ion selectivity. We used a low salt (100 mM KCl) agar bridge in the reference electrode instead of conventional 3 M KCl to prevent contamination of bath with K^+ and respective errors in determinations of the cation selectivity. Therefore, both V_{LJ} at the interfaces between bath and patch pipette ($V_{LJ,1}$) and bath and reference electrode ($V_{LJ,2}$) must be taken into account.

With the open pipette in the bath the electrical potential (V) under zero-current conditions consists of three terms:

$$V = \Delta V - V_{LJ,1} + V_{LJ,2} \quad (1)$$

where ΔV is the electrical potential difference between pipette- and reference AgCl electrodes. The V_{LJ} can be measured (Neher, 1992) or calculated using the generalized Henderson Liquid Junction Potential Equation (Barry & Lynch, 1991). For calculation of V_{LJ} one has to use ion activities instead of concentrations. We used the Debye-Hückel formalism to calculate ion activities which gives an accurate approximation (error <1%) of experimentally measured values (Ammann, 1986) for the determination of mean activity coefficients.

To diminish or even completely eliminate the junction potential between patch electrode and bath ($V_{LJ,1}$), prior to patch formation the solution in the bath always was ''100 KCl'' while the patch pipette contained either ''100 KCl'' or ''15 KCl'' or ''5 $CaCl_2$'' or ''5 $MgCl_2$'' (*see* Table). In all these cases $V_{LJ,1}$ was ⩽2 mV as calculated according to Barry and Lynch (1991). The liquid junction potential between the bath (''100 KCl'') and reference electrodes filled with 100 mM KCl was also close to zero (0.2 mV). So, the potential observed with an open pipette at zero current could be referred to ΔV only which was set to zero before seal formation.

After tight seal formation when the actual measurement under voltage-clamp conditions is initiated there is no more direct contact between patch electrode and bath solutions, thus $V_{LJ,1} = 0$ (Neher, 1992). Therefore, the electrical potential difference across the patch membrane consists of two terms:

$$V = V_{PIP} + V_{LJ,2} \quad (2)$$

Table. Ionic composition of the experimental solutions (all concentrations in mM)

Abbreviation	KCl	$CaCl_2$	$MgCl_2$	HEPES/ KOH	HEPES/ TRIS	pH
''100 KCl''	100	1	5	10		7.5
''15 KCl''	15	1	5	10		7.5
''50 $CaCl_2$''		50			10	7.5
''5 $CaCl_2$''		5			10	7.5
''50 $MgCl_2$''			50		10	7.5
''5 $MgCl_2$''			5		10	7.5

where V_{PIP} is the command potential applied to the patch electrode. Bath solution in our experiments contained ''100 KCl,'' ''50 $CaCl_2$'' or ''50 $MgCl_2$.'' In the last two cases, the calculated values of $V_{LJ,2}$ were rather large, +13.1 mV or +12.8 mV, respectively. The theoretical values were close to those measured under current-clamp conditions, +9.3 ± 0.2 mV ($n = 7$) and +8.3 ± 0.2 mV ($n = 6$) for ''50 $CaCl_2$'' and ''50 $MgCl_2$'' against 100 mM KCl, respectively. The experimentally obtained $V_{LJ,2}$ values were used to calculate the membrane potentials (V) from the applied command potentials (V_{PIP}) according to Eq. 2.

Data Acquisition and Analysis

The records were filtered at 10 kHz by a low pass Bessel filter, digitized using a VR-10B digital data recorder (Instrutech, New York, NY) and stored on videotape. For analysis selected records were filtered and transferred to an IBM-compatible PC. *See* figure legends for filter cutoff frequency and sampling rate. The analyses were carried out with the pClamp 6.0 software package (Axon Instruments).

Results

Selectivity of the Cation Channel in Spinach Thylakoids

Most (163 out of 223, 73%) of the membrane patches isolated from spinach thylakoids contained at least one copy of the ion channel characterized in the present paper. In about 7% of all patches the activity of these channels was accompanied by the activity of other channel types, mainly by the anion-selective channel described previously (Pottosin & Schönknecht, 1995*b*). We selected 88 stable patches where only the dominant channel type was present for further analysis of single channel currents at different ionic conditions. In symmetrical ''100 KCl'' (*see* Table for solutions) the single channel conductance displayed a slight rectification. At negative voltages the slope conductance was 53.0 ± 1.6 pS and at positive voltages 62.3 ± 0.8 pS ($n = 28$, Fig. 1). With ''15 KCl'' solution in the pipette and ''100 KCl'' in the bath the slope conductance decreased to 38.5 ± 2.6 pS ($n = 27$) at positive voltages and at negative voltages asymptotically approached that for sym-

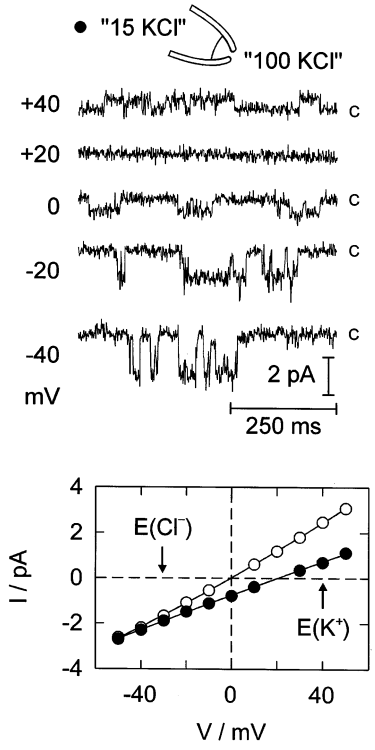

Fig. 1. Cation channel in the thylakoid membrane of spinach. Single channel traces (top) were measured in the inside-out configuration with the stromal side of the thylakoid membrane facing the solution inside the patch pipette. Given voltages refer to the stromal side of the membrane and negative currents correspond to cation influx into the pipette. Original records were filtered at 0.5 kHz and sampled at 1 kHz. The pipette contained the ''15 KCl'' solution and bath the ''100 KCl'' solution (*see* Table). The closed state of the ion channel is indicated by C. Open channel currents were measured either at ''15 KCl''/''100 KCl'' gradient (●, average of 27 patches) or in symmetrical ''100 KCl'' conditions (○, average of 28 patches) and plotted against voltage (bottom). Standard deviation was smaller than symbol size. Solid lines are low-order polynomials fitted to the data. $E(Cl^-)$ and $E(K^+)$ indicate the equilibrium potentials in ''15 KCl''/''100 KCl'' gradient for Cl^- and K^+, respectively.

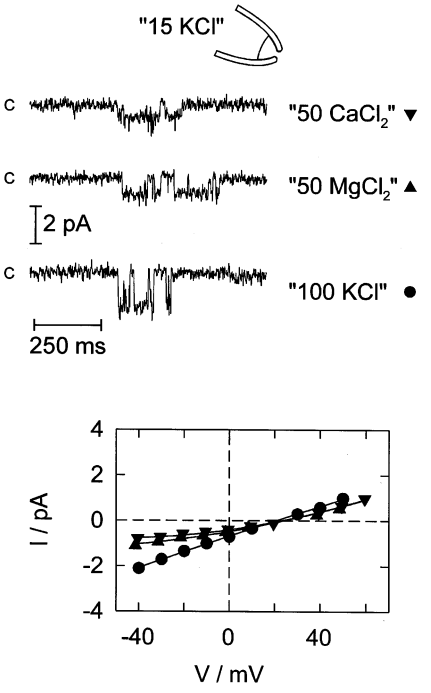

Fig. 2. The thylakoid channel is permeable for divalent cations. Patch pipette was filled with ''15 KCl'' solution, bath contained ''50 $CaCl_2$'' (▼), ''50 $MgCl_2$'' (▲), or ''100 KCl'' (●). Single channel traces (from top to bottom) were measured at −42, −41, and −40 mV (after correction for liquid junction potentials), respectively. Original records were filtered at 0.5 kHz and sampled at 1 kHz. The closed state of the ion channel is indicated by C. Open channel currents were plotted *vs.* membrane voltage (bottom). Solid lines are low-order polynomials fitted to the data.

metrical ''100 KCl''. A negative single-channel current was observed at 0 mV, implying a preference for cations over Cl^- (Fig. 1). The reversal potential was V_R = +20.5 ± 0.4 mV compared to the K^+ equilibrium potential of $E(K^+)$ = +40 mV, the Cl^- equilibrium potential of $E(Cl^-)$ = −31 mV, and equilibrium potentials close to 0 mV for divalent cations (Ca^{2+} and Mg^{2+}), under these conditions.

With ''15 KCl'' in the pipette and either ''50 $CaCl_2$'' or ''50 $MgCl_2$'' in the bath (Fig. 2), the equilibrium potentials for K^+ and Cl^- were both negative. However, the reversal potential for the single channel current remained positive, +22.5 ± 1.1 mV (n = 5) with ''50 $MgCl_2$'' and +23.6 ± 0.9 mV (n = 3) with ''50 $CaCl_2$''. Comparison with the equilibrium potentials for Ca^{2+} (+45 mV) and Mg^{2+} (+25 mV) points to a significant permeability of the channel for divalent cations. The substitution of ''100 KCl'' in the bath either by ''50 $CaCl_2$'' or by ''50 $MgCl_2$'' caused a decrease of the inwardly directed single channel current (Fig. 2).

For further measurements the pipette was filled either with ''5 $CaCl_2$'' or with ''5 $MgCl_2$'', while the bath contained ''100 KCl'' (Fig. 3). This means a very large positive equilibrium potential for K^+, an equilibrium potential close to 0 mV for divalent cations, and $E(Cl^-)$ = −60 mV. The reversal potential was about +28 mV (V_R = +28.2 ± 0.4 mV, n = 12 for ''5 $CaCl_2$''/''100 KCl'' and V_R = +27.8 ± 0.7 mV, n = 15 for ''5 $MgCl_2$''/''100 KCl''). Compared to the ''15 KCl''/''100 KCl'' gradient (V_R = +20.5 mV) the reversal potential was about 10 mV more positive (*cf.* Figs. 3 and 1) i.e., was shifted in the direction of $E(K^+)$. The large concentration gradient for permeant cations (''5 $CaCl_2$'' or ''5 $MgCl_2$'' in the pipette and ''100 KCl'' in the bath; open symbols in Fig. 3) resulted in an obvious rectification of single channel currents. At positive voltages we estimated (by linear regression) a single channel conductance of about 21 pS and 24 pS for ''5 $CaCl_2$'' and ''5 $MgCl_2$'' respectively. At voltages more negative than −30 mV the single chan-

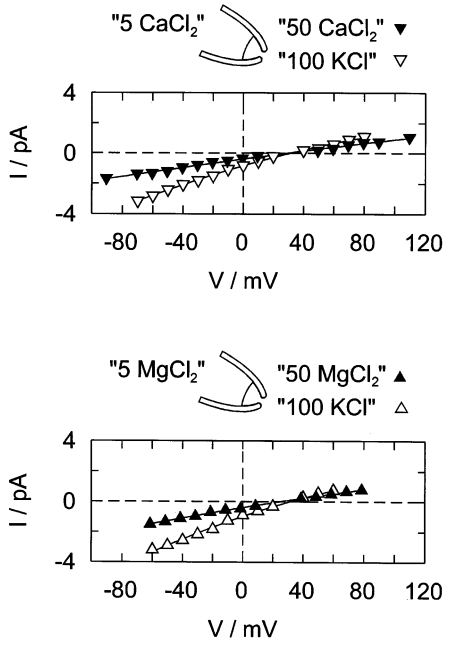

Fig. 3. The thylakoid cation channel is impermeable for Cl^-. Current-voltage relationships of the single channel currents. The pipette was filled with ''5 $CaCl_2$'' (top) or ''5 $MgCl_2$'' (bottom) solution, the bath initially contained ''100 KCl'' (▽ or △) which was replaced by ''50 $CaCl_2$'' (▼) or ''50 $MgCl_2$'' (▲) respectively. Solid lines are low-order polynomials fitted to the data.

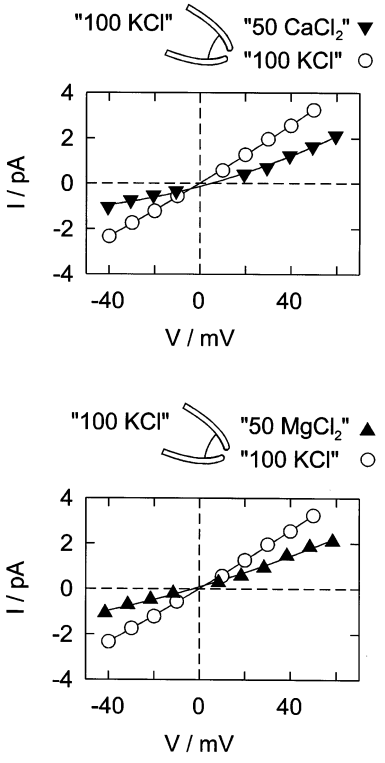

Fig. 4. The thylakoid cation channel has a comparable permeability for K^+ and divalent cations. Current-voltage relationships of the single channel current. Patch pipette and bath were initially filled with ''100 KCl'' solution (○). The bath was replaced either by ''50 $CaCl_2$'' (▼) or by ''50 $MgCl_2$'' (△). Top and bottom current-voltage plots were obtained in the same experiment. Solid lines are low-order polynomials fitted to the data.

nel currents had the same amplitude as under symmetrical ''100 KCl''. In order to estimate the relative permeability of the channel for divalent cations and Cl^-, pure gradients of $CaCl_2$ and $MgCl_2$ were examined. With either ''5 $CaCl_2$'' or ''5 $MgCl_2$'' in the pipette the bath solution was changed from ''100 KCl'' to ''50 $CaCl_2$'' or ''50 $MgCl_2$'' (Fig. 3). This caused a substantial decrease of inward currents (18.6 ± 1.2 pS; $n = 5$ for ''50 $CaCl_2$'' and 19.2 ± 1.7 pS; $n = 6$ for ''50 $MgCl_2$'') and a decrease by roughly one third of the outward currents (13 pS and 15 pS as estimated by linear regression for ''5 $CaCl_2$'' and ''5 $MgCl_2$'', respectively), but no large changes in V_R. The reversal potential values were V_R = +26.1 ± 1.2 mV with a pure $CaCl_2$ gradient and V_R = +26.4 ± 1.0 mV with a pure $MgCl_2$ gradient. These values came close to the equilibrium potentials for Ca^{2+} and Mg^{2+} (+22.5 and +22.8 mV, after correction for ionic activities) but were different from the equilibrium potential for Cl^- (−56 mV). The reversal potential measurements indicated no significant Cl^- permeability of the channel.

Finally, we examined *I/V* relationships of the thylakoid cation channel with ''100 KCl'' in the patch pipette and either ''50 $CaCl_2$'' or ''50 $MgCl_2$'' in the bath (Fig. 4). Under these conditions the equilibrium potential for K^+ was very large and negative and the equilibrium potential for divalent cations was positive (with $E(Ca^{2+})$ = +49 mV; with $E(Mg^{2+})$ = +29 mV). The reversal potentials were V_R = +6.3 ± 1.4 mV (''50 $CaCl_2$'', $n = 6$) and V_R = −2.7 ± 1.0 mV (''50 $MgCl_2$'', $n = 4$). This indicates that the cation channel has comparable permeabilities for K^+, Ca^{2+}, and Mg^{2+}. Under bi-ionic conditions the relative permeability of divalent cations (Cat^{2+}) to K^+ can be calculated from reversal potential values (V_R) according to the following formula (Hille, 1992):

$$V_R = \frac{-RT}{2 \cdot F} \cdot \ln\left(4 \cdot \frac{p_{Cat^{2+}}}{p_{K^+}} \cdot \frac{a_{Cat^{2+}}}{a_{K^+}}\right) \quad (3)$$

where a_i is the activity and p_i the permeability of the respective ion, and R, T, and F have the usual meaning. Using Eq. 3, relative permeabilities for Ca^{2+}/K^+ of 1.93 and for Mg^{2+}/K^+ of 0.93 were calculated. For this calculation the small contribution of divalent cations inside the patch pipette were neglected and thus the relative permeability for divalent cations was slightly underestimated. At negative voltages we estimated (by linear regression) slope conductances of 23.2 ± 1.6 pS and 28.4

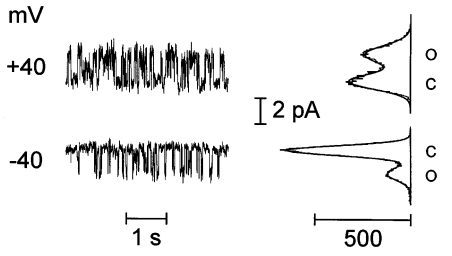

Fig. 5. Voltage dependent kinetics of the cation-selective channel in spinach thylakoids. Single channel traces (filtered at 0.3 kHz and sampled at 1 kHz) at the left and corresponding all-points amplitude histograms (for the whole 20 sec records at each potential) at the right. For all-points amplitude histograms points were binned in 0.05 pA steps and the bar below the histograms indicates 500 points per bin. Measurements were performed with an isolated inside-out patch bathed in symmetrical ''100 KCl'' solution. Closed and open channel states are indicated by C and O, respectively. Amplitude histograms were fitted by a sum of two Gaussian distributions (solid lines).

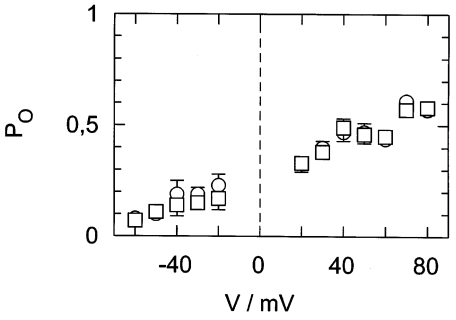

Fig. 6. Voltage dependence of total open probability (P_O) of the thylakoid cation channel P_O (○) was either calculated from all-points amplitude histograms (*compare* Fig. 5) or from idealized single channel traces (events lists, □). In each case calculations were based on 10–20 sec records at each potential. Where error bars are given (on one side only for clarity) 3–9 measurements were averaged.

± 2.0 pS for ''50 $CaCl_2$'' and ''50 $MgCl_2$'' respectively. At positive voltages the slope conductance decreased by about one third when ''100 KCl'' in the bath was exchanged by ''50 $CaCl_2$'' or ''50 $MgCl_2$''. According to the reversal potential measurements the channel displayed an at least twofold higher selectivity for Ca^{2+} relative to K^+. Though, the conductance for Ca^{2+} was about twofold lower than for K^+ resulting in an outward rectification of the *I/V* curve (Fig. 4, top).

Voltage Dependence of the Cation-selective Channel

Patches ($n = 10$) containing only one copy of the cation-selective channel and displaying stable single channel activity for a sufficiently long time (tens of seconds at each given potential) in symmetrical ''100 KCl'' were selected for further kinetic analysis. Potentials above 50 mV were generally not applicable as they, with a few exceptions, caused breakdown of the seal.

An example of voltage-dependent kinetics of the cation channel is shown in Fig. 5. When the membrane potential was changed from +40 to −40 mV channel activity decreased. This is illustrated by a decrease of the open state peak of the corresponding all-points amplitude histograms at the right. The probability to find the channel in the open state (*total open probability*, P_O) corresponds to the relative area of the open state peak. This area was quantified by fitting all-points amplitude histograms with a sum of two Gaussian distributions and P_O was plotted as a function of the applied membrane voltage (Fig. 6, circles). Alternatively, from idealized single channel traces events lists can be constructed which give the duration and amplitude for each open and closed event, and P_O can be calculated from these events

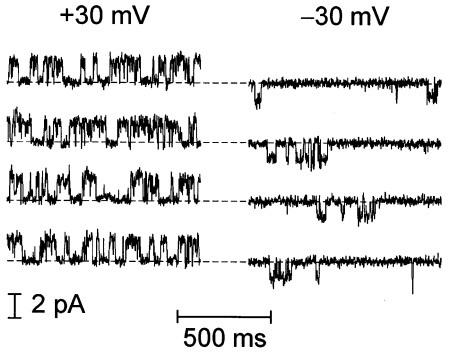

Fig. 7. Example of bursting behavior of the thylakoid cation channel. Consecutive single channel traces at +30 mV (left) and −30 mV (right) are shown. Records were filtered at 0.5 kHz and sampled at 1 kHz. The closed state is indicated by a broken line. Measurements were performed on an isolated inside-out patch bathed in symmetrical ''100 KCl'' solution.

lists (Fig. 6, squares). The two data sets reflecting the voltage-dependence of P_O based on all-points amplitude histograms and on event lists respectively did not differ within the experimental error (Fig. 6). This demonstrates that the idealized single channel traces contained all information necessary to unravel the voltage dependence of the open probability. Therefore, we used the resulting events lists for further kinetic analysis.

The channel displayed complex kinetics. In the single channel records presented in Fig. 7 one can see groups of fast closed-open transitions (bursts) separated by relatively long closures (tens to hundreds of milliseconds, more obvious at negative potentials). This means that at least two different time components are needed to describe the closed times distributions of the cation channel. Kinetic analysis of the records at +40 and −40 mV presented in Fig. 5 was performed and the results are shown in Fig. 8. It revealed three components in the

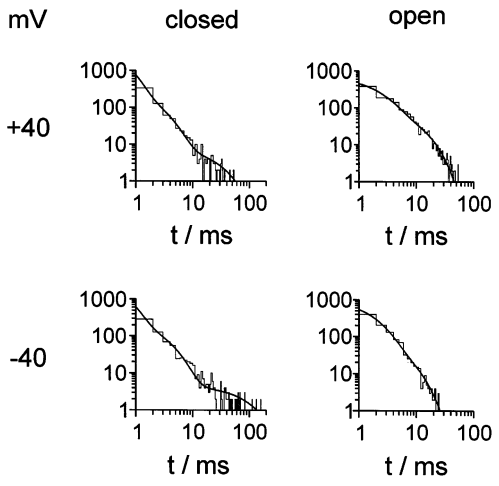

Fig. 8. Dwell times distributions of the thylakoid cation channel. Double-logarithmic plots of the number of events (Y-axis) with a certain duration (X-axis) were based on events lists of the records presented in Fig. 5. They were filtered at 1.5 kHz and sampled at 3 kHz. The dwell times distributions were fitted by a sum of exponential terms, three for the closed times (left) and two for the open times (right). For closed times distributions the following characteristic times (and relative amplitudes) were obtained: at +40 mV: $\tau_1 = 0.41 \pm 0.03$ msec ($A_1 = 0.747$), $\tau_2 = 2.1 \pm 0.02$ msec ($A_2 = 0.190$), $\tau_3 = 26.7 \pm 0.01$ msec ($A_3 = 0.063$); at −40 mV: $\tau_1 = 0.41 \pm 0.03$ msec ($A_1 = 0.648$), $\tau_2 = 2.7 \pm 0.01$ msec ($A_2 = 0.221$), $\tau_3 = 88.9 \pm 0.01$ msec ($A_3 = 0.130$), and for open times distributions at +40 mV: $\tau_1 = 1.6 \pm 0.08$ msec ($A_1 = 0.500$), $\tau_2 = 8.6 \pm 0.02$ msec ($A_2 = 0.500$); at −40 mV: $\tau_1 = 1.5 \pm 0.04$ msec ($A_1 = 0.748$), $\tau_2 = 6.0 \pm 0.01$ msec ($A_2 = 0.252$).

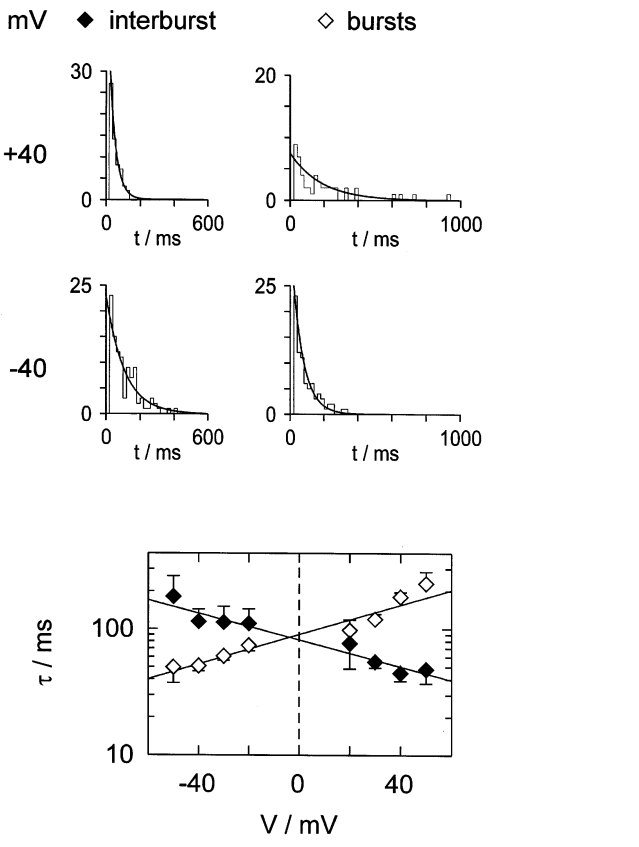

Fig. 9. Burst analysis. Distributions of interburst (top, left) and burst durations (top, right) from the same experiment as in Figs. 5 and 7. Events lists were constructed from 20-sec records at each potential (0.3 kHz sampling rate). The minimum interburst interval was 24 msec. The number (Y-axis) of interburst intervals and bursts with a certain duration (X-axis) were plotted and fitted with monoexponential functions (solid lines). Characteristic times of interburst intervals (◆) were 36.3 msec and 107.9 msec, and of burst durations (◇) 183.2 msec and 62.4 msec for +40 and −40 mV, respectively. Averaged characteristic times (means ± SD, 3–9 measurements) were plotted as a function of membrane voltage in semilogarithmic coordinates (bottom). The datapoints were fitted by Eq. 5 (solid lines). This yielded the following parameters: for interburst intervals (τ_1, ◆) $z_I = -0.31 \pm 0.033$ and $\tau_I(0) = 82.1 \pm 3.91$ msec; for burst durations (τ_B, ◇) $z_B = 0.35 \pm 0.041$ and $\tau_B(0) = 90.6 \pm 5.02$ msec.

closed times distributions and two components in the open times distributions (Fig. 8). Only the slower components in dwell times distributions displayed a significant dependence on the applied voltage. The durations of fast transitions within a burst and of long closed times separating bursts differed by at least one order of magnitude (*compare* legend of Fig. 8).

On this basis we performed a burst analysis. For this purpose a minimum interburst interval is taken and all consecutive closures shorter than this interval were summed up in a single burst. With this definition of a burst, the *probability of bursts* (P_B) and the *open probability within bursts* (P_I) can be estimated. When multiplied with each other P_B and P_I give the *total open probability* (P_O):

$$P_O = P_B \cdot P_I. \quad (4)$$

It is obvious that a proper estimation of the minimum interburst interval is critical for a correct burst analysis. One way to do this estimation is to analyze the number of closures per burst as a function of the test interburst interval (Sigurdson et al., 1987). As the minimum interburst interval approaches the ''true'' value the number of closings per burst will be relatively insensitive to further increase of this interval. When our records made in the voltage range from −50 to +50 mV were analyzed in such a manner minimum interburst intervals between 20 and 30 msec were obtained. This corresponds to the lower limit for the slowest closed times component estimated by the kinetic analysis presented in Fig. 8.

On the basis of these minimum interburst intervals, from the sample presented in Fig. 5 durations of bursts and interburst intervals were estimated and the resulting time distributions were fitted by monoexponential functions (Fig. 9, top) to yield the characteristic times. This analysis was performed for different membrane voltages

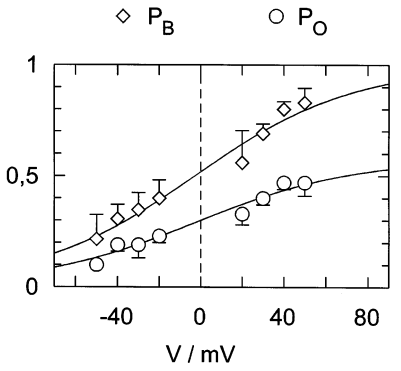

Fig. 10. Comparison of the *total open probability* (P_O, ○) and the *probability of bursts* (P_B, ◇) for the cation-selective channel in spinach thylakoids. All measurements were performed on isolated inside-out patches bathed in symmetrical ''100 KCl'' solution. The *probability of bursts* (P_B) was calculated from the data presented in Fig. 9 (bottom) using Eq. 6. The *total open probability* (P_O) was calculated from all-points amplitude histograms (*see* Fig. 6). P_B and P_O were obtained from the same experimental series (points are means ± SD from 3–9 measurements). The voltage dependence of P_O and P_B was fitted simultaneously according to Eqs. 4 and 7 (solid lines). This yielded P_I = 0.58 ± 0.03, V_B = −3 ± 2 mV and z = 0.66 ± 0.04.

applied. The averaged values of the characteristic times of burst durations (τ_B) and interburst intervals (τ_I) for nine patches are presented as a function of membrane potential in Fig. 9, bottom. While the burst duration increased with increasing voltages the interburst interval decreased. The voltage-dependencies were described by (Fig. 9):

$$\tau_B(V) = \tau_B(0) \cdot \exp\left(z_B \cdot \frac{F}{RT} \cdot V\right) \text{ and } \tau_I(V) = \tau_I(0) \cdot \exp\left(z_I \cdot \frac{F}{RT} \cdot V\right) \quad (5)$$

where z_B and z_I are the valencies of the respective gating charges. They were estimated by nonlinear regression analysis as z_B = +0.35 and z_I = −0.31. From the time constants of burst durations (τ_B) and interburst intervals (τ_I) we calculated the *probability of bursts* (P_B) as:

$$P_B = \frac{\tau_B}{\tau_B + \tau_I} \quad (6)$$

In Fig. 10 the voltage-dependence of the *probability of bursts* (P_B) based on Eq. 6 was compared with the voltage dependence of the *total open probability* (P_O) based on all-points amplitude histograms (Figs. 5 and 6). The voltage-dependence of P_B was described by a Boltzmann distribution in the form:

$$P_B(V) = \left[1 + \exp\left(z \cdot \frac{F}{RT} \cdot (V_B - V)\right)\right]^{-1} \quad (7)$$

where $z = z_B - z_I$ and V_B is the voltage at which P_B = 0.5 (Fig. 10). The values estimated by nonlinear regression analysis were z = 0.66 and V_B = −3 mV. According to Eq. 4 the *total open probability* (P_O) is the product of the *probability of bursts* (P_B) and the *open probability within bursts* (P_I). The voltage-dependence of P_B is obvious. It remains to be tested whether there is a significant voltage-dependence of P_I or whether P_I is constant and the observed voltage-dependence of P_O reflects solely the voltage-dependence of P_B. On the basis of the definition of bursts given above (separated by intervals longer than the minimum interburst interval) the *open probability within a burst* (P_I) was calculated from event lists. This yielded values between P_I = 0.64 (−50 mV) and P_I = 0.74 (+50 mV) indicating that P_I was hardly voltage-dependent. Accordingly $P_O(V)$ as fitted by a Boltzmann distribution (Eq. 7) multiplied with a constant factor (P_I = const; Eq. 4). Fitting $P_O(V)$ by the product of two Bolzmann distributions, assuming P_I is voltage-dependent, consistently resulted in a very small voltage dependence (z = 0.12 ± 0.07) and did not improve the fit. The open probability within a burst (P_I) was hardly voltage-dependent and, therefore, the observed voltage-dependence of the total open probability (P_O) solely reflected the voltage-dependence of burst formation (P_B).

Discussion

Characteristics of the Cation Channel in Native Spinach Thylakoid Membranes

This work demonstrates the existence of a cation-selective channel in spinach thylakoid membranes (Figs. 1 and 2). In pure $CaCl_2$ or $MgCl_2$ gradients, the reversal potential corresponded to the equilibrium potential for the respective divalent cation (Fig. 3) indicating that the cation channel is hardly permeable for Cl^-. Based on reversal potentials, the channel showed a comparable permeability for K^+ and divalent cations. The permeability ratio for Ca^{2+} over K^+ was at least 2.0 and the permeability ratio for Mg^{2+} over K^+ was at least 1.0 (Fig. 4). As tight seal formation was hardly possible in the absence of divalent cations (Pottosin & Schönknecht, 1995*a*) both, bath and pipette always contained at least 5 mM divalent cations (*see* Table). A direct measurement of the Cl^-/K^+ permeability ratio was therefore not possible.

Whenever bi-ionic conditions were applied with divalent cations on one side and (mainly) K^+ on the other side a rectification of single channel currents was observed (Figs. 2–4). Obviously, the single channel conductance was larger for K^+ than for divalent cations, at 100 mM K^+ about 62 pS compared to 21 pS or 24 pS for 50 mM Ca^{2+} or Mg^{2+}, respectively (averaged values from Figs. 3 and 4). When the activity for K^+ was increased by a factor of about five (from 20 mM to 105 mM), the

single channel conductance increased by about 40% (from 38.5 pS to 62 pS). This indicates a relatively high affinity for K^+ (about 20 mM) assuming a Michaelis Menten type of binding. An increase of the Ca^{2+} or Mg^{2+} concentration (to 50 mM in Figs. 2–4) on the lumenal side resulted in a decrease (by about one third) of the cation efflux from the stroma into the lumen. This is especially obvious in Fig. 4 where the outward current was mainly carried by 100 mM K^+. This may be explained in the following way, divalent cations (at higher concentrations) temporarily occlude the channel and thereby reduce the outward current. The slight rectification observed under symmetrical ''100 KCl'' (62 pS for the outward and 53 pS for the inward current) might be explained on this basis by slightly different binding affinities for divalent cations at the lumenal side compared to the stroma face of the channel.

The cation channel of the spinach thylakoid membrane displayed a moderate voltage dependence resulting in an increase of the *total open probability* (P_O) from about 0.1 at −60 mV to 0.6 at +80 mV (Fig. 6). The cation channel had a complex gating behavior (Fig. 7) with at least two characteristic open times and three characteristic closed times (Fig. 8). The observed voltage-dependence was consistently explained by an increased probability for bursts at more positive voltages (Fig. 10) due to decreasing interburst intervals and increasing burst durations (Fig. 9). The open probability within bursts (P_I) was hardly voltage-dependent.

Comparison with Other Cation Channels in Plant Endomembranes

Previous measurements with spinach thylakoid membrane fragments incorporated into planar bilayers (Tester & Blatt, 1988) or giant liposomes (Enz et al., 1993) revealed some cation-selective channels. Tester & Blatt (1988) worked with high KCl concentrations and measured a single-channel conductance of 120 pS in a 1000/300 mM KCl gradient. Enz and coworkers (1993) reported four different ion conductances. First, a weakly Cl^--selective channel was presented which is different from the Cl^- channel in the native spinach thylakoid membrane (Pottosin & Schönknecht 1995*b*) by its selectivity, conductance and gating behavior. Second, a putative K^+ channel with a conductance of 110 pS (at 100 mM KCl plus 5 mM $CaCl_2$) was shown which seems to be specific for K^+ over Ca^{2+}. The high conductance and the low relative Ca^{2+}/K^+ permeability makes this channel different from the cation channel characterized by us. Third and fourth, conductances for Ca^{2+} (20 pS 62 mM Ca^{2+}) and Mg^{2+} (35 pS at 80 mM Mg^{2+}) were presented without a further characterization which might correspond to the cation channel described here. A general problem has to be mentioned regarding reconstitution studies with spinach thylakoid membrane fragments. It was shown that under reconstitution into giant liposomes the channel portion of the thylakoid H^+-ATPase forms nonselective cation channels with some 10–20 pS and higher (30, 60, and 120 pS in 100 mM KCl) conductances. These artificial channels were effectively blocked by 1 μM venturicidin (Schönknecht et al., 1989), a potent inhibitor of F-type ATPases. We have demonstrated that the cation channel measured by patch-clamp technique in the native spinach thylakoid membrane is insensitive to venturicidin up to 10 μM (Pottosin & Schönknecht, 1995*b*). It remains unclear, which of the cation channels observed in reconstitution studies (Tester & Blatt, 1988; Enz et al., 1993) may be related to dearranged membrane spanning subunits of the thylakoid H^+-ATPase.

Cation channels with comparable conductances for Ca^{2+} and Mg^{2+} have been found in the plant vacuolar membrane (Ping, Yabe & Muto, 1992; Allen & Sanders, 1994). Moreover, the so-called slow vacuolar (SV) channel has been reported to have a relative Ca^{2+}/K^+ permeability of about three and a negligible relative Cl^-/K^+ permeability (Ward & Schroeder, 1994; Allen & Sanders, 1995), but see Schulz-Lessdorf & Hedrich (1995) for a different view. When K^+ is replaced by Ca^{2+} at the lumenal side the conductance for the outward K^+ current through the SV channel is decreased by 25% (from 155 pS to 117 pS). Despite a higher relative permeability for Ca^{2+} compared to K^+, single-channel conductance with Ca^{2+} as the only permeant ion dropped to 16 pS (Ward & Schroeder, 1994). Both effects are similar to what we observed with the thylakoid cation channel (Figs. 2–4). It should be noted that even Ca^{2+} channels with a relative Ca^{2+}/K^+ permeability >100 are known to conduct K^+ ions in the absence of divalent cations and normally transport rates for K^+ are much higher compared to divalent cations (Tsien et al., 1987). In this regard, the thylakoid cation channel shares properties of other ion channels permeable for divalent cations.

Physiological Implications of the Thylakoid Membrane Cation Channel

The electrical compensations of light-driven H^+ uptake into thylakoids is known to be achieved by concomitant fluxes of Cl^-, K^+ and Mg^{2+} (Dilley & Vernon, 1965; Hind et al., 1974; Chow, Wagner & Hope, 1976; Krause, 1977). Anions (Cl^- and NO_3^-) are likely to be transported through the thylakoid membrane via the voltage-dependent anion channel found in higher plants, *Peperomia metallica* and *Spinacea oleracea*, as well as in Charophyte alga *Nitellopsis obtusa* (Schönknecht et al., 1988; Pottosin & Schönknecht, 1995*a*,*b*). However, anions alone appear to compensate only part of the light-driven H^+ current. As an example, measurements with

ion-selective microelectrodes in a living plant cell showed that roughly half of the H^+ taken up into chloroplasts after illumination is electrically compensated by anion influx (Thaler, Simonis & Schönknecht, 1993). The remaining part of the charge balance has to be provided by an efflux of cations. Light-dependent cation fluxes across the spinach thylakoid membrane are well documented, although the relative contribution of K^+ and Mg^{2+} is a matter of debate (Dilley & Vernon, 1965; Hind et al., 1974; Barber, 1976; Vredenberg, 1976; Bulychev & Vredenberg, 1976; Krause, 1977; Fang, Mi & Berkowitz, 1995). It was shown that Ca^{2+} and Mg^{2+} ions are transported through the thylakoid membrane via a common pathway showing a slight preference for Ca^{2+} (Hind et al., 1974). Here we demonstrate that the dominant cation channel in spinach thylakoid membranes is almost equally permeable for K^+, Ca^{2+}, and Mg^{2+}. The cation-selective channel described in this paper is likely to explain on the molecular level the different observations about cation permeability of the intact thylakoid membrane of spinach.

There is the question whether the current through this channel is large enough to contribute significantly to the electrical compensation of light-driven H^+ currents. Direct measurements of light-driven H^+ pump activity in thylakoids by patch-clamp technique (Bulychev, Antonov & Schevchenko, 1992; Muniz, Pottosin & Sandoval, 1995) yielded a current density of 0.07 pA/μm^2. Given that a membrane patch has an approximate surface of 10 μm^2 (Hamill et al., 1981) this value transforms to 0.7 pA per patch. The total concentrations of K^+ and Mg^{2+} in chloroplasts (stroma plus lumen) within spinach leaves are kept relatively constant under a broad range of growing conditions, 80–180 mM and 13–18 mM, respectively (Schröppel-Meier & Kaiser, 1988). Therefore, under physiological conditions the current through the thylakoid cation channel is mainly carried by K^+ ions and a single channel conductance close to 60 pS as measured here with symmetrical 105 mM K^+ plus 5 mM Mg^{2+} (Fig. 1) is a good estimate. When light is turned on the electrical potential across the thylakoid membrane transiently reaches a maximum of up to −60 to −80 mV and declines to −10 to −15 mV at steady state (Bulychev et al., 1972; Remiš et al., 1986). The *total open probability* (P_O) of the cation channel measured in this voltage range increased from 0.08 at −60 mV to 0.23 at −20 mV (Fig. 6). Thus, the time-averaged current through a single cation channel is practically constant, −0.29 pA at −60 mV and −0.28 pA at −20 mV. One cation channel per membrane patch is sufficient to compensate about 40% of the light-driven pump current of about 0.7 pA (*see above*). With more than one cation channel per patch, what was frequently observed, the conductance of the cation channel is more than sufficient to electrically compensate light-driven H^+ fluxes.

Another possible function of the thylakoid cation channel concerns Mg^{2+} homeostasis in chloroplasts. After the onset of illumination, Mg^{2+} ions are transported from the thylakoid lumen to the stroma and the concentration of free stromal Mg^{2+} increases by approximately 2 mM (from about 3 to 5 mM) at physiological pH (Krause, 1977; Portis, 1981). As the chloroplast envelope is known to be hardly permeable for Mg^{2+} (Gimmler, Schäfer & Heber, 1974) almost all Mg^{2+} released from thylakoids accumulates in the stroma. Based on relative thylakoid (2 μm^3) *vs.* stroma volumes (30 μm^3) of 1:15 (Heldt et al., 1973), the total Mg^{2+} concentration inside the thylakoid lumen has to decrease by 30 mM to produce a 2-mM increase of the total stromal Mg^{2+} concentration. Taking into account buffering of Mg^{2+}, an increase of the free stromal Mg^{2+} concentration by 2 mM requires even larger changes in total Mg^{2+} concentration. A gradient of 5/50 mM $MgCl_2$ (stroma/lumenal side) corresponding to a single channel conductance of 19 pS (Fig. 3) might come close to physiological conditions. Assuming a membrane potential of −10 mV (Bulychev et al., 1972), a *total open probability* P_O = 0.3 results (Fig. 6). With a density of 1 cation channel per 10 μm^2 and a thylakoid surface of 500 μm^2 (based on 10 to 15 μm bleb diameters) a Mg^{2+} current of −2.9 pA or $3 \cdot 10^{-17}$ mol sec^{-1} across the whole thylakoid membrane can be calculated. For a stromal volume of 30 μm^3 (Heldt et al., 1973) this gives an increase of total stromal Mg^{2+} concentration by about 1 mM sec^{-1}. In other words, the thylakoid cation channel can mediate changes of the free stromal Mg^{2+} concentrations in the millimolar range within a few seconds. Physiological significance of the light-driven Mg^{2+} redistribution in chloroplasts was emphasized by many authors (but *see* Ben-Hayyim (1978) for an alternative point of view). According to Krause (1977) and Portis (1981) stromal concentration of free Mg^{2+} in the dark is low (1–3 mM) and it is roughly doubled under illumination. The light-induced increase of stromal Mg^{2+} apparently occurs in the concentration range where it may activate key enzymes of CO_2 fixation (Portis, 1981; Portis et al., 1977). Barber (1976) speculated that light-induced changes of stromal Mg^{2+} concentrations affect thylakoid stacking and hence the efficiency of energy transfer between photosystems I and II. Thus, the Mg^{2+}-permeable channel in thylakoid membranes could serve as an important element in the feedback control of light-driven processes as well as a link between light and dark photosynthesis reactions.

Conclusions

A dominant channel responsible for transport of mono- and divalent cations was characterized in the native thylakoid membrane from spinach. This channel is prob-

ably involved in the electrical compensation of light-driven H^+ uptake into thylakoids. Compared to K^+, Mg^{2+} fluxes through this channel are likely to play a minor role in charge balancing whereas the channel-mediated increase of the stromal Mg^{2+} concentration after illumination may have an important regulatory effect on photosynthesis. The channel described in this paper had only a moderate voltage-dependence compared to classical voltage-dependent channels (Hille, 1992) and compared to the thylakoid anion channel (Pottosin & Schönknecht, 1995*a*). There should be additional mechanisms to regulate the thylakoid cation channel activity.

We thank Dr. U. Heber for generous support and Dr. W. Simonis for helpful discussions. This work was financially supported by the Deutsche Forschungsgemeinschaft (SFB 176 TP B11) and by a research fellowship from the Alexander von Humboldt Foundation to I.I. Pottosin.

References

Allen, G.J., Sanders, D. 1994. Two voltage-gated, calcium release channels coreside in the vacuolar membrane of broad bean guard cells. *Plant Cell* **6:**685–694

Allen, G.J., Sanders, D. 1995. Calcineurin, a type 2B protein phosphatase, modulates Ca^{2+}-permeable slow vacuolar ion channel of stomatal guard cells. *Plant Cell* **7:**1473–1483

Ammann, D. 1986. Ion-selective Microelectrodes. Springer-Verlag, New York

Azzone, G., Benz, R., Bertl, A., Colombini, M., Crofts, A., Dilley, R., Dimroth, P., Dutton, P.L., Felle, H., Harold, F., Junge, W., Kaback, H.R., Knaff, D., Krulwich, T., Lodish, H., Malmström, B., Maloney, P., Mannella, C., Padan, E., Papa, S., Rottenberg, H., Rudnick, G., Rydström, J., Silverstein, T., Skulachev, V., Slayman, C., Tedeschi, H., Wikström, M., Wilson, T.H. 1993. Transmembrane measurements across bioenergetic membranes. *Biochim. Biophys. Acta* **1183:**1–3

Barber, J. 1976. Ionic regulation in intact chloroplasts and its effect on primary photosynthetic processes. *In:* Topics in Photosynthesis: The Intact Chloroplast. J. Barber, editor. pp. 89–134. Elsevier, New York

Barry, P.H., Lynch, W.J. 1991. Liquid junction potentials and small cell effects in patch-clamp analysis. *J. Membrane Biol.* **121:**101–117

Ben-Hayyim, G. 1978. Mg^{2+} translocation across the thylakoid membrane: studies using the ionophore A23187. *Eur. J. Biochem.* **83:**99–104

Bulychev, A.A., Andrianov, V.K., Kurella, G.A., Litvin, F.F. 1972. Microelectrode measurements of the transmembrane potential of chloroplasts and its photoinduced changes. *Nature* **236:**175–177

Bulychev, A.A., Vredenberg, W.J. 1976. The effect of cations and membrane permeability modifying agents on the dark kinetics of the photoelectric response in isolated chloroplasts. *Biochim. Biophys. Acta* **423:**548–556

Bulychev, A.A., Antonov, V.F., Schevchenko, E.V. 1992. Patch-clamp studies of light-induced currents across the thylakoid membrane of isolated chloroplasts. *Biochim. Biophys. Acta* **1099:**16–24

Chow, W.S., Wagner, G., Hope, A.B. 1976. Light-dependent redistribution of ions in isolated spinach chloroplasts. *Aust. J. Plant Physiol.* **3:**570–575

Dilley, R.A., Vernon, L.P. 1965. Ion and water transport processes related to the light-dependent shrinkage of spinach chloroplasts. *Arch. Biochem. Biophys.* **111:**365–375

Enz, C., Steinkamp, T., Wagner, R. 1993. Ion channels in the thylakoid membrane (a patch-clamp study). *Biochim. Biophys. Acta* **1143:**67–76

Fang, Z., Mi, F., Berkowitz, G.A. 1995. Molecular and physiological analysis of a thylakoid K^+ channel protein. *Plant Physiol.* **108:** 1725–1734

Gimmler, H., Schäfer, G., Heber, U. 1974. Low permeability of the chloroplast envelope towards cations. *In:* Proceedings of the IIIrd International Congress on Photosynthesis Research, M. Avron, editor. Vol. 3, pp. 1381–1392. Elsevier, Amsterdam

Hamill, O.P., Marty, A., Neher, E., Sakmann, B., Sigworth, F.J. 1981. Improved patch-clamp techniques for high-resolution recordings from the cells and cell-free membrane patches. *Pfluegers Arch.* **391:**85–100

Heldt, H.W., Werdan, K., Milovancev, M., Geller, G. 1973. Alkalinization of the chloroplast stroma caused by light-dependent proton flux into the thylakoid lumen. *Biochim. Biophys. Acta* **314:**224–241

Hille, B. 1992. Ionic Channels of Excitable Membranes, Second Edition. Sinauer Associates, Sunderland, Massachusetts

Hind, G., Nakatani, H.Y., Izawa, S. 1974. Light-dependent redistribution of ions in suspensions of chloroplast thylakoid membranes. *Proc. Natl. Acad. Sci. USA* **71:**1484–1488

Junge, W., Jackson, B. 1982. The development of electrochemical potential gradients across photosynthetic membranes. *In:* Photosynthesis: Energy Conversion in Plants and Bacteria. Govindjee, editor. Vol. I, pp. 589–646. Academic Press, New York

Krause, G.H. 1977. Light-induced movement of magnesium ions in intact chloroplasts. Spectroscopic determination with eriochrome blue SE. *Biochim. Biophys. Acta* **460:**500–510

Muniz, J., Pottosin, I.I., Sandoval, L. 1995. Patch-clamp study of vascular plant chloroplasts: single channels and photocurrents. *J. Bioenerg. Biomembr.* **27:**249–258

Neher, E. 1992. Correction for liquid junction potentials in patch clamp experiments. *Methods Enzymol.* **207:**123–131

Ping, Z., Yabe, I., Muto, S. 1992. Identification of K^+, Cl^-, and Ca^{2+} channels in the vacuolar membrane of tobacco cell suspension cultures. *Protoplasma* **171:**7–18

Portis, A.R. 1981. Evidence of a low stromal Mg^{2+} concentration in intact chloroplasts in the dark. *Plant Physiol.* **67:**985–989

Portis, A.R., Chon, C.J., Mosbach, A., Heldt, H.W. 1977. Fructose- and sedoheptulose-bisphosphatase. The site of a possible control of CO_2 fixation by light-dependent changes of the stromal Mg^{2+} concentration. *Biochim. Biophys. Acta* **461:**313–325

Pottosin, I.I., Schönknecht, G. 1995*a*. Patch-clamp study of the voltage-dependent anion channel in the thylakoid membrane. *J. Membrane Biol.* **148:**145–158

Pottosin, I.I., Schönknecht, G. 1995*b*. Anion and cation channels in the thylakoid membrane. *In:* Photosynthesis: From Light to Biosphere. P. Mathis, editor. Vol. III. pp. 99–102. Kluwer Academic Publishers, Dordrecht

Remiš, D., Bulychev, A.A., Kurella, G.A. 1986. The electrical and chemical components of the protonmotive force in chloroplasts as measured with capillary and pH-sensitive microelectrodes. *Biochim. Biophys. Acta* **852:**68–73

Schönknecht, G., Hedrich, R., Junge, W., Raschke, K. 1988. A voltage-dependent chloride channel in the photosynthetic membrane of a higher plant. *Nature* **336:**589–592

Schönknecht, G., Althoff, G., Apley, E.C., Wagner, R., Junge, W. 1989. Cation channels by subunit III of the channel portion of the chloroplast H^+-ATPase. *FEBS Lett.* **258:**190–194

Schröppel-Meier, G., Kaiser, W.M. 1988. Ion homeostasis in chloroplasts under salinity and mineral deficiency I. Solute concentrations in leaves and chloroplasts from spinach plants under NaCl or $NaNO_3$ salinity. *Plant Physiol.* **87:**822–827

Schulz-Lessdorf, B., Hedrich, R. 1995. Protons and calcium modulate SV-type channels in the vacuolar-lysosomal compartment-channel interaction with calmodulin inhibitors. *Planta* **197:**655–671

Sigurdson, W.J., Morris, C.E., Brezden, B.L., Gardner, D.R. 1987. Stretch activation of a K^+ channel in molluscan heart cells. *J. Exp. Biol.* **127:**191–209

Thaler, M., Simonis, W., Schönknecht, G. 1993. Light-dependent changes of the cytoplasmic H^+ and Cl^- activity in the green alga *Eremosphaera viridis. Plant Physiol.* **99:**103–110

Tester, M., Blatt, M.R. 1989. Direct measurements of K^+ channels in thylakoid membranes by incorporation of vesicles into planar lipid bilayers. *Plant Physiol.* **91:**249–252

Tsien, R.W., Hess, P., McCleskey, E.W., Rosenberg, R.L. 1987. Calcium channels: mechanisms of selectivity, permeation, and block. *Annu. Rev. Biophys. Chem.* **16:**265–290

Vredenberg, W.J. 1976. Electrical interactions and gradients between chloroplast compartments and cytoplasm. *In:* Topics in Photosynthesis: The Intact Chloroplast. J. Barber, editor. pp. 53–58. Elsevier, New York

Ward, J.M., Schroeder, J.I. 1994. Calcium-activated K^+ channels and calcium-induced calcium release by slow vacuolar ion channels in guard cell vacuoles implicated in the control of stomatal closure. *Plant Cell* **6:**669–683